

NASA Technical Paper 1109

**Cold-Air Performance
of a Tip Turbine Designed
To Drive a Lift Fan**

**III - Effect of Simulated Fan
Leakage on Turbine Performance**

Jeffrey E. Haas, Milton G. Kofskey,
Glen M. Hotz, and Samuel M. Futral, Jr.

JANUARY 1978

NASA

NASA Technical Paper 1109

Cold-Air Performance
of a Tip Turbine Designed
To Drive a Lift Fan

III - Effect of Simulated Fan
Leakage on Turbine Performance

Jeffrey E. Haas

Propulsion Laboratory

U.S. Army R&T Laboratories (AVRADCOM)

Milton G. Kofskey, Glen M. Hotz,
and Samuel M. Futral, Jr.

Lewis Research Center
Cleveland, Ohio



National Aeronautics
and Space Administration

**Scientific and Technical
Information Office**

1978

COLD-AIR PERFORMANCE OF A TIP TURBINE DESIGNED TO DRIVE A LIFT FAN

III - EFFECT OF SIMULATED FAN LEAKAGE ON TURBINE PERFORMANCE

by Jeffrey E. Haas*, Milton G. Kofskey, Glen M. Hotz, and Samuel M. Futral, Jr.

Lewis Research Center

SUMMARY

Performance data were obtained experimentally for a 0.4 linear scale version of the LF460 lift fan turbine for a range of scroll inlet total to diffuser exit static pressure ratios at design equivalent speed with simulated fan leakage air. Performance results were obtained for full and partial admission operation.

A static efficiency decrease of 14.2 percent was obtained at a scroll inlet total to diffuser exit static pressure ratio of 4.1 with full admission operation and leakage air fractions of 5 percent at the rotor inlet and 5 percent at the rotor exit. This efficiency decrease was attributed to blockage effects and mixing and windage losses associated with the leakage air. When the leakage air rates at the rotor inlet and exit were varied separately, the static efficiency decreased about 2 percent for each percent increase in rotor inlet leakage air and about 1 percent for each percent increase in rotor exit leakage air.

A static efficiency decrease of about 2.5 percent was obtained at a scroll inlet total to diffuser exit static pressure ratio of 4.1 with partial admission operation and 5 percent rotor inlet and 5 percent rotor exit leakage air. A substantially smaller efficiency decrease with partial admission operation was attributed to the fact that only about 20 to 40 percent of the leakage air was bled into the active side of the turbine during partial admission operation.

The primary mass flow through the turbine during both full and partial admission operation was not affected by the leakage air.

INTRODUCTION

In the past several years a need has been recognized for an airplane that has the VTOL capability of a helicopter together with the advantages of the current conventional

*Propulsion Laboratory, U.S. Army R&T Laboratories (AVRADCOM).

aircraft with respect to speed, cargo capacity, and fuel economy. Using the V/STOL aircraft for civil aviation would reduce the congestion and noise pollution that exists at many large airports. For military service, the V/STOL aircraft could be used for assault transport, antisubmarine warfare, search and rescue missions, and early warning systems.

Several engine and component arrangements have been considered for providing takeoff and landing lift for this type of aircraft. These are discussed in some detail in references 1 to 3. One arrangement is a fan driven by a turbine that is mounted on the rotating shroud of the fan blades. Such a turbine is called a tip turbine and is supplied by one or more remotely located gas generators.

In order to make trade-off studies of the various lift fan drive systems, detailed performance data for the tip turbine are required. However, at present, only minimal performance data exist.

Reference 4 is the detailed design report of a lift fan program sponsored by the NASA Lewis Research Center. This particular lift fan system design, which has the designation LF460, uses a tip turbine to drive the fan. Because of the need for detailed performance data for tip turbines, a scale version of the tip turbine from the LF460 was fabricated and tested. A linear scale factor of 0.4 was chosen so that an existing Lewis Research Center cold-air component test facility could be used. A solid disk was used in place of the fan for the test rotor. The rotor clearances were scaled to match the calculated hot running clearances of the full-scale turbine. Three series of tests were planned. The first tests were general performance tests, the results of which are presented in reference 5. These tests were conducted over a range of speeds from 40 to 140 percent of the equivalent design speed and over a range of scroll inlet total to diffuser exit static pressure ratios from 2.0 to 4.2. At the design values of equivalent speed and stator inlet total to rotor exit total pressure ratio, the efficiency was 0.815 as compared to the design value of 0.832.

The second series consisted of partial admission tests with one side of the turbine scroll used at a time to simulate loss of one of the gas generators. The results are presented in reference 6. These tests were conducted in two parts. Each part had an admission arc of 180° . The tests were conducted over a range of speeds from 40 to 140 percent of equivalent design speed and over a range of scroll inlet total to diffuser exit static pressure ratios from 2.2 to 5.0. At the design values of equivalent speed and stator inlet total to rotor exit total pressure ratio, an average partial admission efficiency of 0.740 was obtained.

The performance results from the third tests in which air simulating fan leakage air was bled into the turbine at the rotor inlet hub and the rotor exit hub is presented in this report. Since a solid rotor disk was used in place of the fan for the test rotor, the leakage air was supplied through separate air lines and was bled into the turbine

airstream from plenum chambers located on either side of the rotor disk.

Performance tests were made at design equivalent speed for both full and partial admission operation. For both modes of operation data were obtained over a range of scroll inlet total to diffuser exit static pressure ratios of approximately 2.0 to 4.8 with three separate combinations of rotor inlet and rotor exit leakage air. In addition, for full admission operation, the scroll inlet total to diffuser exit static pressure ratio was maintained constant at the design value of 4.1 and the rotor inlet and rotor exit leakage air rates were varied independently. In all of these tests the ratio of turbine inlet to simulated fan leakage air total temperature was approximately 1.1.

In this report, results are presented as curves relating equivalent values of mass flow, torque, and efficiency with pressure ratio and leakage air. Also included are the trends in efficiency with leakage air when the turbine was operated at design equivalent speed and at a constant turbine pressure ratio.

SYMBOLS

C_p	specific heat, J/(kg)(k)
Δh	turbine specific work, J/g
L	leakage fraction, ratio of leakage flow to turbine airflow
N	rotative speed, rpm
p	absolute pressure, N/cm ²
T	absolute temperature, K
U	blade velocity, m/sec
V	absolute gas velocity, m/sec
ΔV_u	change in absolute tangential velocity, m/sec
W	relative gas velocity, m/sec
w	mass flow, kg/sec
α	absolute gas flow angle measured from axial direction, deg
β	relative gas flow angle measured from axial direction, deg
Γ	torque, N-m
$\Delta\Gamma$	decrease in torque, N-m
γ	ratio of specific heats
δ	ratio of scroll inlet total pressure to U.S. standard sea-level pressure, p_1/p^*

- ϵ function of γ used in relating parameters to those using air inlet conditions at U. S. standard sea-level conditions, $(0.740/\gamma)[(\gamma + 1)/2]^{\gamma/(\gamma-1)}$
- η static efficiency based on pressure ratio p'_1/p_6
- $\Delta\eta$ decrease in static efficiency
- θ_{cr} squared ratio of critical velocity at scroll inlet temperature to critical velocity at U. S. standard sea-level temperature $(v_{cr1}/v_{cr}^*)^2$
- ρ density, kg/m^3

Subscripts:

- cr critical corresponding to Mach number at unity
- eq equivalent
- 1 station at scroll inlet (fig. 12)
- 3 station at stator inlet (fig. 12)
- 4 station at stator exit and/or rotor inlet (fig. 12)
- 5 station at rotor exit (fig. 12)
- 6 station at diffuser exit (fig. 12)

Superscripts:

- ' absolute total state
- * U. S. standard sea-level conditions (temperature, 288.16 K; pressure, 10.13 N/cm^2)

TURBINE DESCRIPTION

A brief description of the full-scale turbine will be followed by a description of the scale-model turbine. Engine design conditions for the full-scale turbine are presented in table I along with the design equivalent conditions for the scaled turbine.

Full-Scale Turbine

General description. - The full-scale turbine was designed to drive a lift-fan having a nominal tip diameter of 152.4 centimeters. Figure 1 (from ref. 4) presents the basic layout of the fan and drive turbine. The two inlets to the scroll are adjacent to each other. Each inlet is supplied by a separate gas generator and, in turn, each inlet supplies a different 180° segment of the scroll. The purpose of the dual inlets is for

redundancy in case one of the gas generators fails.

Figure 1 shows axial and radial clearances in the turbine that are large compared to a conventional turbine design. Unusually large radial clearances are the result of the large thermal growth of the scroll structure. The large axial clearances are needed to accommodate the considerable flexure of the fan. A three-chamber scroll was used to distribute the hot gas in the stator and to form a compact, structurally sound design. The lift-fan system was designed to be compact so that it could be enclosed within the envelope of the wing cross section. A turbine exit diffuser was used to produce as low a static pressure as possible in the turbine rotor to prevent leakage of hot turbine gas into the fan.

Figure 2 shows the design mean-section velocity diagrams for the turbine. As discussed in reference 4, the single-stage turbine was designed to include a supersonic stator and a subsonic, zero static pressure drop rotor. The turbine rotor had a hub to tip radius ratio of about 0.94. Both the stator and rotor bladings were of constant section design.

Scroll. - The layout of the scroll flowpath is shown in figure 3. As discussed in reference 4, the scroll is divided in half with each half supplied by separate inlets which are located adjacent to each other. This results in an airflow direction which is the same as the direction of rotor rotation in one-half of the scroll. This half of the scroll is called the forward side. In the other half of the scroll the airflow is in a direction opposite to that of rotation. This half of the scroll is called the reverse side. Figure 4 shows the relationship of the forward and reverse sides to the direction of rotation. Each half is independent of the other, and each serves 180° of the stator arc.

At each inlet the scroll is divided into three chambers. Only the large upper chamber continues around the full 180° . The design Mach number for the flow entering the scroll is approximately 0.3. The flow is then turned in the circumferential direction, divided into three chambers on each side, and accelerated to a Mach number of about 0.35. The flow then passes through a cascade of struts; these struts turn the flow radially into a vaneless annulus, which turns the flow axially into the stator assembly.

Stator. - Since the flow in one-half of the scroll moves counter to the direction of rotation, three different vane profiles are used to meet the varying flow angles created by the scroll. Figure 5 shows the vane types and how they are located circumferentially with respect to the scroll. The vane profiles were designed for inlet flow angles of 60° , 0° , and -60° . However, the diverging portions of the passages were geometrically similar for all three types of vanes. The vanes were designed with a convergent-divergent flow passage, which resulted in an exit to throat area ratio of 1.071. There were 42 type I vanes, 38 type II vanes, and 77 type III vanes for a total of 157 vanes.

Rotor. - Figure 6 shows the rotor blade profile. There were 264 rotor blades. The rotor profile is constant from hub to tip. The rotor was designed to operate at impulse conditions to minimize the tip leakage losses. As mentioned previously, large axial and radial clearances were associated with fan flexure and shroud growth. The tip clearance is of the order of 1.3 centimeters, which is approximately 25 percent of the rotor blade height. Thus, impulse blading with shrouded blade tips was chosen to minimize the tip leakage losses.

Diffuser. - The exit diffuser (fig. 1) consists of a diverging annular passage with eight hollow struts. The struts serve as structural members to support the fan structure. For the test turbine the rotor exit fan leakage air passed through these hollow struts to a plenum chamber located downstream of the rotor disk. The exit to inlet area ratio of the diffuser was approximately 1.5.

Scale-Model Turbine

In order to test the LF460 turbine in an existing Lewis Research Center cold-air component test facility, it was necessary to design and fabricate a 0.4 linear scale model of this turbine. Figure 7 is a photograph of the scaled turbine installed in the test cell. The photograph was taken from the exhaust end. Visible in this photograph are the inlet and exhaust piping and the scroll assembly.

Figure 8 is a closeup of the scroll and stator assembly on its mounting stand. The trailing edge of some of the stator vanes can be seen in this figure. The scroll chambers of the scaled turbine were rectangular rather than circular as in the full-size turbine. This change was made in order to simplify the fabrication.

The rotor is shown in figure 9. The rotor disk and blading were machined from a single forging, and a shroud ring was furnace-brazed to the blade tips. As discussed in the INTRODUCTION, the axial and radial tip clearances were scaled from the hot operating condition for the full-scale turbine.

APPARATUS

The apparatus consisted of the turbine, a cradled gearbox, and a cradled dynamometer to absorb the power output of the turbine and to control turbine speed. In addition, inlet and exhaust piping with flow controls was used to set the inlet and exit pressures of the turbine. The arrangement of the apparatus is shown schematically in figure 10. Dry pressurized air was supplied from a central air system. The air passed through a 100-kilowatt heater, a calibrated orifice plate, and a remotely controlled turbine inlet valve. Two valves, one in each of the two scroll inlets, were used

to direct the air into the scroll. The air was exhausted from the turbine through a system of piping and a remotely operated valve into a central low-pressure exhaust system. A 224-kilowatt dynamometer cradled on hydrostatic trunion bearings was used to absorb the turbine power, to control the turbine speed, and to measure the torque. The dynamometer was coupled to the turbine shafting through a gearbox on hydrostatic bearings. The gearbox provided relative rotative speeds between the dynamometer and turbine of 1.0 to 2.0. The stators of the gearbox and dynamometer were coupled so that the measured torque was the net torque developed by the turbine. Figure 11 shows the dynamometer and gearbox.

Since a solid disk was used in place of the fan for the test rotor, room air was drawn into the turbine to simulate fan leakage air. The rotor inlet and rotor exit leakage air passed through separate pressure regulators and venturi flowmeters into separate manifolds. Six feedlines ran from one manifold to six equally spaced locations around the front side of the turbine housing. The rotor inlet leakage air passed through these feedlines to a plenum chamber on the upstream side of the rotor disk. Eight feedlines ran from the other manifold to the eight hollow diffuser struts. The rotor exit leakage air passed through these feedlines to a plenum chamber on the downstream side of the rotor disk. From these two plenum chambers the leakage air was bled into the turbine airstream at the rotor inlet hub and rotor exit hub. Figure 7 shows the rotor exit leakage air manifold and its eight feedlines. For simplicity the leakage air manifolds and feedlines are not shown in figure 10.

INSTRUMENTATION

A torque arm attached to the dynamometer stator and a commercial strain-gage load cell were used to measure the net turbine torque. The load cell output was read on a digital voltmeter. The rotational speed was detected by a magnetic pickup and a shaft-mounted gear. The magnetic pickup output was converted to a direct-current voltage, which was proportional to the frequency, and fed into the digital voltmeter.

State conditions of the flow were determined by measurements taken at the scroll and stator inlets and rotor and diffuser exits. The instrumentation stations and the type of instrumentation at each station are shown in figures 12 and 13. The instrumentation at the scroll inlet (station 1) included four static pressure taps in each of the two inlets. A total temperature rake containing three thermocouples was also located upstream of the two inlets. At the stator inlet (station 3) there were six static pressure taps equally spaced circumferentially around the turbine along the hub wall. There were also six total pressure probes spaced circumferentially around the turbine. Each total pressure probe contained three elements to provide measurements at the mean

radius and near the hub and tip walls. In addition, there was a tube on each side of the mean-section total pressure sensing tube. These two side tubes, which had their sensing ends cut off to form a 90° wedge, were connected to a differential pressure transducer to provide a means for manually alining the probe with the flow. A scale and pointer were attached to each probe to provide an indication of the mean-section flow angle.

At the rotor exit (station 5) there were nine single-element shielded (Kiel-type) total pressure probes approximately evenly spaced circumferentially. These probes were spaced radially so that there were three each near the hub wall, the mean radius, and the tip wall. Use of Kiel-type total pressure probes provided accurate total pressure readings over a range of absolute flow angle misalignments of about $\pm 30^\circ$.

At the diffuser exit (station 6) there were eight static pressure taps equally spaced circumferentially with four each at the inner and outer walls. Two self-alining probes, located 180° apart at the mean radius, were used for measuring total pressure, total temperature, and flow angle.

For the partial admission tests with leakage air the turbine airflow only went through half of the turbine at a time. Therefore, only the instrumentation readings on the side of the turbine with the airflow were used for data reduction.

PROCEDURE

Performance tests with leakage air were made at design equivalent speed for both full and partial admission operation. For both modes of operation data were obtained at nominal scroll inlet total conditions of 330 K and 9.60 newtons per square centimeter over a range of scroll inlet total to diffuser exit static pressure ratios of approximately 2.0 to 4.8 with three separate combinations of rotor inlet and rotor exit leakage air. Expressed as percentages of the turbine airflow, these three combinations were (1) 0-percent rotor inlet and 5-percent rotor exit leakage air, (2) 5-percent rotor inlet and 0-percent rotor exit leakage air, and (3) 5-percent rotor inlet and 5-percent rotor exit leakage air.

In addition, for full admission operation, the scroll inlet total to diffuser exit static pressure ratio was maintained constant at the design value of 4.1, while the rotor inlet and rotor exit leakage air rates were varied separately. In all of these tests the ratio of the turbine inlet total temperature to the leakage air total temperature was approximately 1.1. For these tests only the leakage air into the turbine was investigated. In addition, with partial admission operation the leakage air was bled into both the active and inactive sides of the turbine. In the event one of the gas generators supplying the tip turbine failed, the leakage air would not be restricted to only the active side of the turbine.

A dynamometer torque calibration was obtained before each daily series of runs. Corrections were applied to the measured net turbine torque to include the effects of calculated disk windage (assuming no leakage air) and measured turbine bearing friction to obtain the turbine aerodynamic torque.

In this investigation the turbine was rated on the basis of static efficiency η . The static efficiency was defined as

$$\eta = \frac{\frac{2\pi\Gamma N}{60}}{w_p C_p T_1 \left[1 - \left(\frac{p_6}{p_1'} \right)^{(\gamma-1)/\gamma} \right]}$$

RESULTS AND DISCUSSION

Performance results are presented for a 0.4 linear scale version of the LF460 lift fan turbine with simulated fan leakage air. These performance tests were conducted at design equivalent speed for full and partial admission operation. For both modes of operation the data were obtained at nominal scroll inlet total conditions of 330 K and 9.60 newtons per square centimeter over a range of scroll inlet total to diffuser exit static pressure ratios of approximately 2.0 to 4.8 with three separate combinations of rotor inlet and rotor exit leakage air. Expressed as percentages of the turbine airflow, these three cases were (1) 0-percent rotor inlet and 5-percent rotor exit leakage air (case II), (2) 5-percent rotor inlet and 0-percent rotor exit leakage air (case III), and (3) 5-percent rotor inlet and 5-percent rotor exit leakage air (case IV). The results from either reference 5 or 6 are used as the zero leakage air case (case I).

In addition, for full admission operation the scroll inlet total to diffuser exit static pressure ratio was maintained constant at the design value of 4.1 and the rotor inlet and rotor exit leakage air rates were varied separately. In all of these tests the ratio of the turbine inlet total temperature to the leakage air total temperature was approximately 1.1.

Performance results are presented as curves relating equivalent values of mass flow, torque, and efficiency with pressure ratio and leakage air. Also included are the trends in efficiency with leakage air when the turbine was operated at design equivalent speed and at the design scroll inlet total to diffuser exit static pressure ratio of 4.1.

LEAKAGE AIR WITH FULL ADMISSION

Mass Flow

Figure 14 shows the variation of equivalent mass flow $\epsilon w \sqrt{\theta_{cr}} / \delta$ with pressure ratio p_1'/p_6 and leakage air L_4 and L_5 . This figure indicates that the stator was choked at an equivalent mass flow of 3.110 kilograms per second. This was within 0.50 percent of the reference 5 mass flow rate. The scatter shown in the data represented less than 1 percent of the measured mass flow. This was considered to be within the experimental accuracy of the mass flow measurement. Therefore, it was concluded that the leakage air did not affect the choking mass flow rate.

Torque

Figure 15 shows the variation of equivalent torque $\epsilon \Gamma / \delta$ with pressure ratio p_1'/p_6 and leakage air L_4 and L_5 . This figure shows that as the total amount of leakage air increased the torque decreased. If the case I torque is used as a reference, the decreases in torque at the design pressure ratio of 4.1 for cases II, III, and IV were 2.5, 9.1, and 14.2 percent, respectively. These decreases in torque with leakage air were attributed to blockage effects and mixing losses associated with the leakage air injection and to windage losses associated with the leakage air flowing along both faces of the rotor disk prior to entering the turbine flow path.

Figure 16 shows the relative magnitude of these losses at the design pressure ratio of 4.1. The windage losses were calculated using the model of reference 7. The blockage effects and mixing losses were determined with the aid of the turbine off-design computer program of reference 8.

Since a solid rotor disk was used in place of the fan in the test rotor, windage losses occurred because the rotor disk imparted part of its torque energy to create angular momentum in the leakage air. These windage losses were not accounted for in the disk windage correction that was added to the measured dynamometer torque. To estimate the windage losses associated with the leakage air, the modified friction loss equations of reference 7 for the case of the rotating disk with throughflow were used. The ratio of the angular velocity of the leakage air to the angular velocity of the disk was assumed to be 0.45. Figure 16 shows the magnitude of these windage losses. The windage losses accounted for 44, 11, and 15 percent of the torque decrease for cases II, III, and IV, respectively. Since these windage losses would not occur in the actual full-scale turbine, their effect had to be accounted for in determining the actual loss associated with the leakage air.

When the windage losses were subtracted from the total losses due to the leakage

air, the remaining loss results from blockage effects and mixing losses in the turbine flow path. Even though the comparison of the torque losses for the three leakage air cases was made at the same scroll inlet total to diffuser exit static pressure ratio, the blockage effects and mixing losses caused changes in the expansion ratios across the stator and rotor and, thus, differences in torque. Since static pressures were not measured at the stator and rotor exits, an iterative method was used to calculate the rotor exit static pressure for the three leakage air cases. These calculated pressure ratios, together with the computer program of reference 8, were then used to analyze the blockage effects and mixing losses.

For case II it was assumed that the leakage air only caused an increase or decrease in the stator exit and rotor exit static pressures due to additional mass flow passing through the diffuser. Based on the iterative calculation procedure stated previously, an increase in the rotor exit static pressure of about 4 percent from the case I value was indicated. The reference 8 computer program was used to generate a curve of torque as a function of rotor exit static pressure. This curve is presented in figure 17 where the rotor exit static pressure is ratioed to the stator inlet total pressure. This curve shows that a 4-percent increase in the rotor exit static pressure would cause a torque decrease of about 1.4 percent (point B in fig. 17). Therefore, the calculated windage loss and the change in the rotor exit static pressure reasonably explained the torque decrease observed for case II.

For case III, the leakage air caused a blockage in the rotor, thus causing a reduction in the annulus area available to the turbine primary mass flow. This blockage caused a redistribution in the split in reaction between the stator and rotor. In addition, mixing loss and secondary flow losses could also have occurred which would cause additional changes in reaction.

The continuity equation was used to approximate the blockage caused by the rotor inlet leakage air. The blockage caused by the injection of a given amount of leakage flow into the main flow stream was related by the mass flow per unit area (ρV) of the two flows. For case III the ratio of the ρV of the primary mass flow to the ρV of the leakage air was approximately 1.8. Therefore, for 5-percent leakage air a blockage in the rotor of 9 percent resulted.

The reference 8 computer program was again used to generate another curve of torque as a function of rotor exit static pressure with a blockage factor equal to 9 percent of the rotor annulus area and with no change in the loss model from case II. This curve is also shown in figure 17. This curve and the calculated rotor exit static pressure for case III indicated a torque decrease from case I of about 8 percent (point C in fig. 17). Thus, the use of 9-percent blockage appeared to account for the observed torque decrease for case III. It should be noted that the consideration of only the blockage caused by the leakage air ignored the effect of any mixing on secondary flow losses

as well as any torque benefit from the leakage air caused by the leakage air doing useful work in the rotor. The possibility exists for this turbine that any torque benefit from the leakage air was just equal to the mixing and secondary flow losses caused by the leakage air injection, thus allowing for the results observed.

For case IV, the calculated rotor exit static pressure was approximately 15 percent less than it was for case I. However, at this static pressure and for the 9-percent blockage curve, the torque decrease from case I was less than that shown in figure 16 (point D in fig. 17). The reference 8 computer program indicated that a blockage factor of approximately 11 percent would be necessary to account for all of the torque decrease (point F in fig. 17). If no interaction is assumed between the rotor inlet and rotor exit leakage air, the blockage factor should be the same for cases III and IV. Thus, a torque curve based on a blockage factor of 10 percent (represented by a mean line in the hatched area between the 9- and 11-percent blockage factor curves in fig. 17) and the calculated rotor exit static pressure would give agreement with the measured torque value within 1 percent.

Figure 18 shows the variation of static efficiency η with pressure ratio p'_1/p_6 and leakage air L_4 and L_5 . The definition of the static efficiency was given in the PROCEDURE section. In this definition only the turbine primary mass flow was used. Since the mass flow was constant for the different leakage air cases, the efficiency was proportional to the torque at a given pressure ratio. Therefore, at the design pressure ratio of 4.1, the percent decrease in efficiency for the three leakage air cases corresponded to the percent decrease in torque noted in the previous section. Thus, using the case I efficiency as a reference, the decreases in efficiency at the design pressure ratio for cases II, III, and IV were 2.5, 9.1, and 14.2 percent, respectively. After correcting for the windage losses, the decreases in efficiency for cases II, III, and IV were 1.4, 8.0, and 11.8 percent, respectively.

Figure 19 shows the percent decrease in static efficiency $\Delta\eta/\eta$ as the leakage air was varied from 0 to about 6 percent of the turbine primary flow at the design scroll inlet total to diffuser exit static pressure ratio of 4.1. Figure 19(a) shows the decrease in efficiency with rotor exit leakage air with 0-percent rotor inlet leakage air. Conversely, figure 19(b) shows the decrease in efficiency with rotor inlet leakage air with 0-percent rotor exit leakage air. Figure 19(a) shows that between a rotor exit leakage air fraction of 0 and about 2.5 percent there was essentially no change in the efficiency. Beyond 2.5 percent there was an approximate 1-percent decrease in efficiency with each percent increase in the rotor exit leakage air. Figure 19(b) indicates that there was an approximate 2-percent decrease in efficiency with each percent increase in the rotor inlet leakage air from 0- to about 6-percent leakage air. The results from this figure can be used to provide an approximate indication of the efficiency decrease that occurs for various combinations of rotor inlet and rotor exit leakage air.

LEAKAGE AIR WITH PARTIAL ADMISSION

Mass Flow

Figure 20 shows the variation of equivalent mass flow with pressure ratio and leakage air for partial admission operation. The choking mass flows obtained with both modes of partial admission operation were within 0.25 percent of the reference 7 values. As with full admission operation (fig. 13), the leakage air did not affect the mass flow rate.

Torque

Figure 21 shows the variation of equivalent partial admission torque with pressure ratio and leakage air. This figure indicates that the decrease in torque with leakage air was much smaller for partial admission operation than for full admission operation. If the case I partial admission torque is used as a reference, the decreases in torque for both modes of partial admission operation at the design pressure ratio of 4.1 were 0, 1.5, and 2.5 percent for cases II, III, and IV, respectively. Correcting these decreases for the amount caused by the windage loss resulted in torque decreases of 0, 0.5, and 1.0 percent for cases II, III, and IV, respectively.

These small decreases in partial admission torque are explained in the following manner. As described in the PROCEDURE section, the leakage air was bled into the rotor inlet and rotor exit plenum chambers with no provision for controlling the split of leakage air between the active and inactive sides. Thus, the leakage air sought the path of lower resistance through the turbine. For case II, it appeared that little or no leakage air passed through the active side of the turbine. Figure 19(a) indicates that the leakage air fraction in the active side could have ranged from 0 to 0.020 (or 0 to 40 percent of the total leakage air) without a measurable effect on the partial admission torque.

For case III, figure 19(b) indicates that a leakage air fraction of 0.009 (or 20 percent of the total leakage air) in the active side of the turbine could have caused a torque decrease from case I of 0.5 percent. This appears to indicate that there was a rather large discrepancy in the leakage fraction passing through the active side of the turbine for cases II and III. Since the conditions controlling the split of leakage air between the active and inactive sides were similar for cases II and III, it was expected that the same leakage air fractions should have occurred. Therefore, one of the following two hypotheses could have occurred. First, since figure 19(a) indicated a leakage air fraction ranging from 0 to 0.020 for case II and figure 19(b) indicated a leakage air fraction of 0.009 for case III, the amount of leakage air being bled into the active side

for cases II and III was about 20 percent of the total leakage air. The second hypothesis was that as much as 40 percent of the total leakage air was bled into the active side for cases II and III. In this event, it would have to be assumed for case III that since there was more leakage air in the active side than was indicated by figure 19(b) the leakage flow passing through the rotor in the inactive side must have produced enough torque to counteract the torque decrease caused by the leakage air passing through the active side. Insufficient data existed to determine which hypothesis was more probable.

For case IV, the slight additional torque decrease from case III was unexpected, since figure 19(a) showed that the rotor exit leakage air had no effect on the partial admission torque. One possible explanation is that there was some torque benefit from the leakage air in the inactive side of the turbine for case III and that the addition of rotor exit leakage air going from case III to case IV reduced this torque benefit, thereby causing the additional torque decrease for case IV. If this explanation is valid, this would tend to confirm the second of the two hypothesis mentioned earlier for the amount of leakage air bled into the active side of the turbine for cases II and III.

Turbine Efficiency

Figure 22 shows the variation of static efficiency with pressure ratio and leakage air. As with full admission operation the percentage decreases in efficiency for cases II, III, and IV for partial admission operation corresponded to the respective percentage decreases in torque. It should be noted that the efficiency curves for case I for both modes of partial admission operation are unpublished data from the investigation reported in reference 6.

SUMMARY OF RESULTS

The performance was obtained for a 0.4 linear scale version of the LF460 lift fan turbine over a range of scroll inlet total to diffuser exit static pressure ratios at design equivalent speed with simulated fan leakage air. Performance results were obtained for both full and partial admission operation. The results of this investigation may be summarized as follows:

1. A static efficiency decrease of 14.2 percent was obtained at a scroll inlet total to diffuser exit static pressure ratio of 4.1 with full admission operation and 5-percent rotor inlet and 5-percent rotor exit leakage air. This efficiency decrease was attributed to blockage effects and mixing and windage losses associated with the leakage air.
2. When the rotor inlet and rotor exit leakage air rates were varied separately,

the static efficiency decreased by about 2 percent for each percent increase in rotor inlet leakage air and about 1 percent for each percent increase in rotor exit leakage air.

3. A static efficiency decrease of about 2.5 percent was obtained at a scroll inlet total to diffuser exit static pressure ratio of 4.1 with partial admission operation and 5-percent rotor inlet and 5-percent rotor exit leakage air. This much smaller efficiency decrease was attributed to the fact that only about 20 to 40 percent of the leakage air was bled into the active side of the turbine during partial admission operation.

4. The primary mass flow through the turbine during both full and partial admission operation was not affected by the leakage air.

Lewis Research Center,
National Aeronautics and Space Administration,
Cleveland, Ohio, October 14, 1977,
505-05.

REFERENCES

1. Novak, Lloyd R.: The Lift/Cruise Fan Multimission V/STOL Aircraft. AIAA Paper 75-277, Feb. 1975.
2. Dugan, James F., Jr.; et al.: Preliminary Study of an Air Generator - Remote Lift Fan System for VTOL Transports. NASA TM X-67916, 1971.
3. Gertsma, L. W.; and Zigan, S.: Propulsion System for Research VTOL Transports. ASME Paper 73-GT-24, Apr. 1973.
4. LF460 Detail Design. (71-AEG-297, General Electric Co.; NASA Contract NAS2-6056.) NASA CR-120787, 1971.
5. Haas, Jeffrey E.; et al.: Cold-Air Performance of a Tip Turbine Designed to Drive a Lift Fan. I - Baseline Performance. NASA TM X-3452, 1976.
6. Haas, Jeffrey E.; et al.: Cold-Air Performance of a Tip Turbine Designed to Drive a Lift Fan. II - Partial Admission. NASA TM X-3481, 1977.
7. Turbine Design and Application, Vol. II. NASA SP-290, 1973, pp. 131-138.
8. Flagg, E. E.: Analytical Procedure and Computer Program for Determining the Off-Design Performance of Axial Flow Turbines. NASA CR-710, 1967.

TABLE I. - TURBINE DESIGN CONDITIONS

Parameter	Engine (full scale)	Equivalent (0.4 scale)
Stator inlet temperature, T_3 , K	1 144	288.2
Stator inlet pressure, p_3 , N/cm ²	37.7	10.13
Mass flow rate, w , kg/sec	34.6	3.03
Rotative speed, N , rpm	4 300	5395
Specific work, Δh , J/g	268.4	67.6
Torque, Γ , N-m	20 623	363
Power, kW	9 290	205
Pressure ratio, p_3/p_5	3.05	3.16
Pressure ratio, p_1/p_6	3.92	4.10
Efficiency, η'	0.832	0.832
Work factor, $\Delta V_u/U$	1.982	1.982

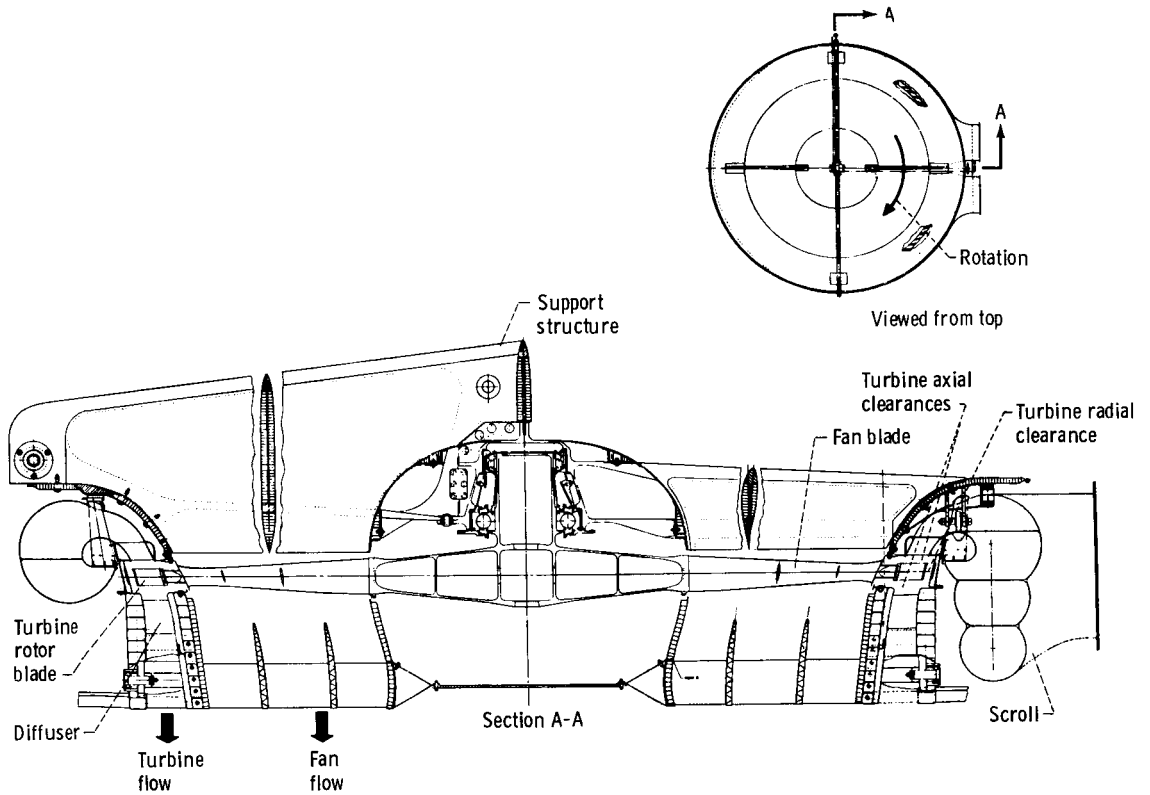
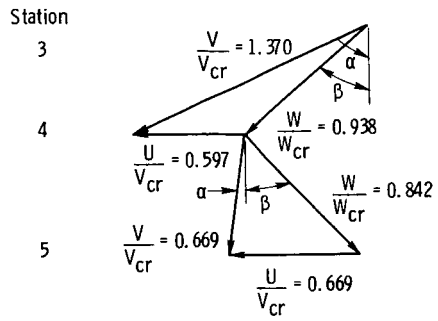


Figure 1. - Lift-fan assembly.



Station 4 66.3° 50.0°
 Station 5 7.3° -43.0°

Figure 2. - Design velocity diagrams for LF460 turbine at mean section.

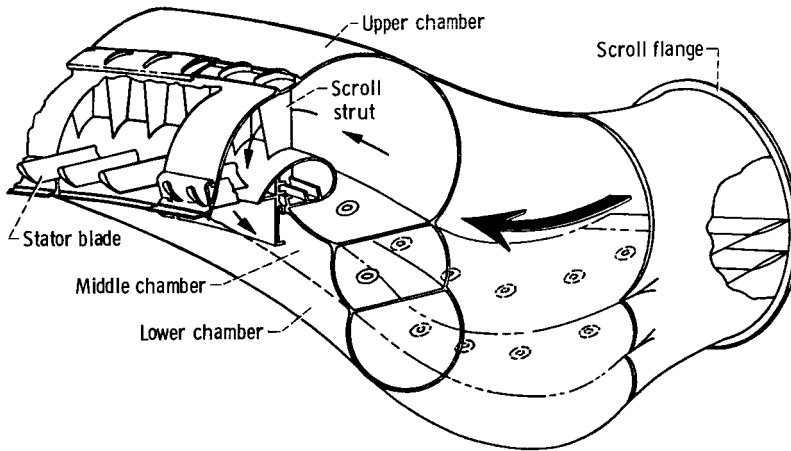


Figure 3. - Scroll flowpath.

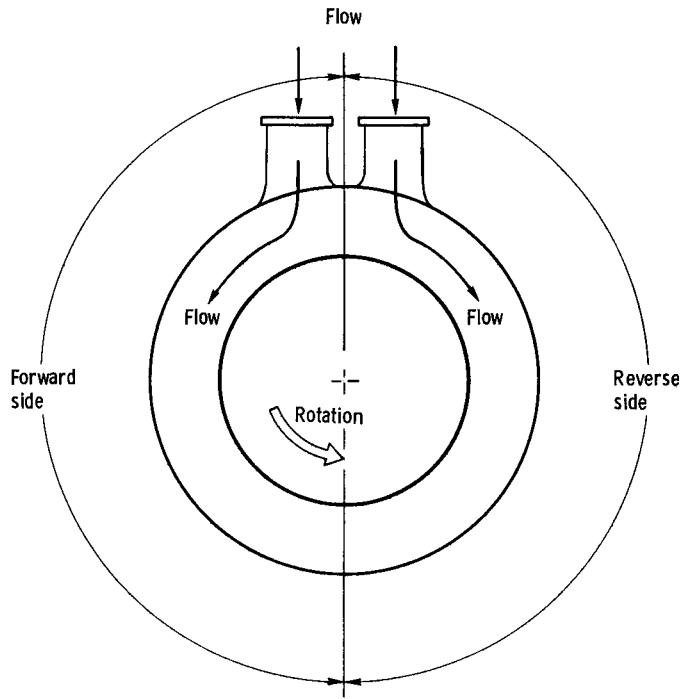


Figure 4. - Sketch showing forward and reverse sides of turbine (viewed from exhaust end).

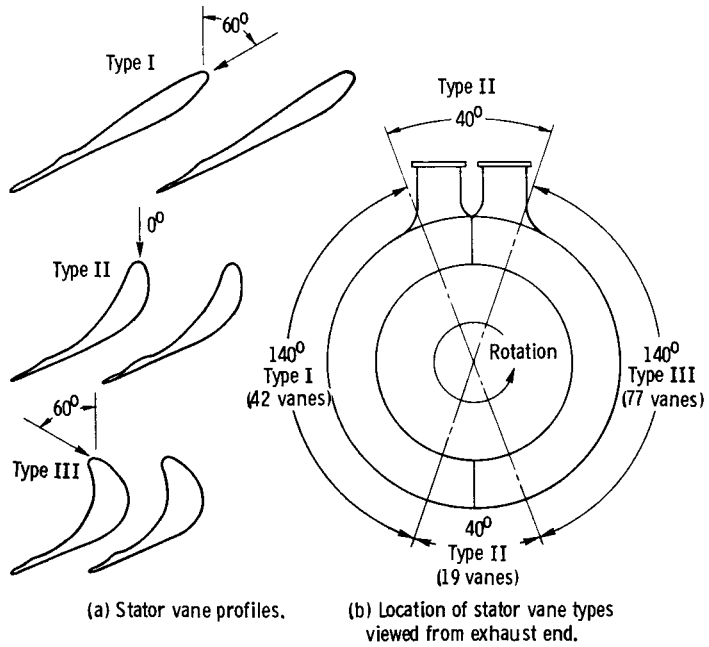


Figure 5. - Sketch showing stator vane profiles and locations.

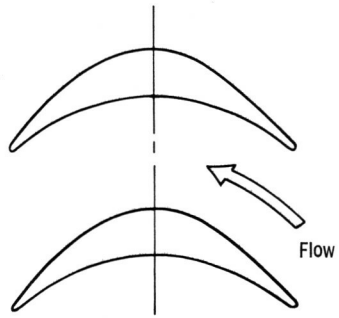


Figure 6. - Rotor blade profile.

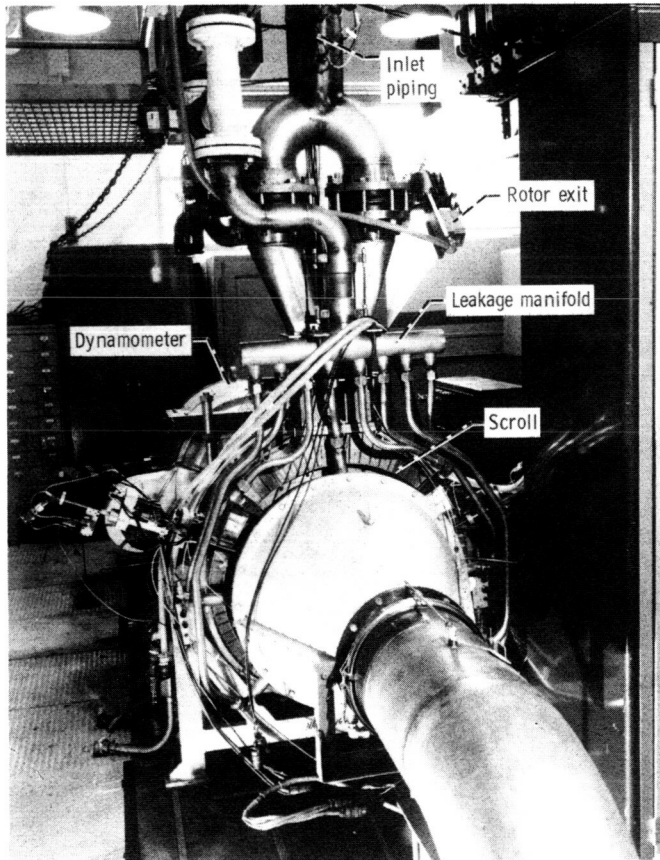


Figure 7. - Turbine test installation.

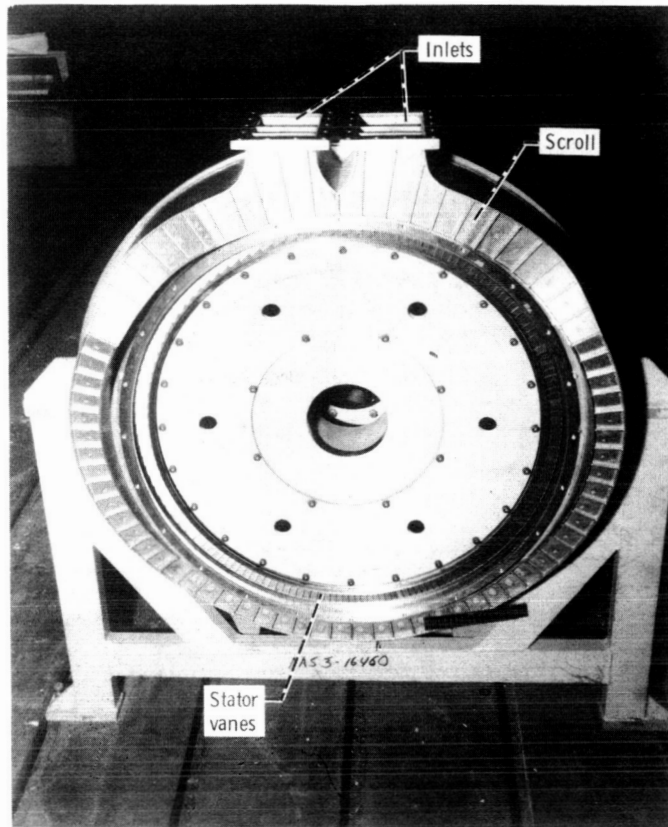


Figure 8. - Test scroll and stator.

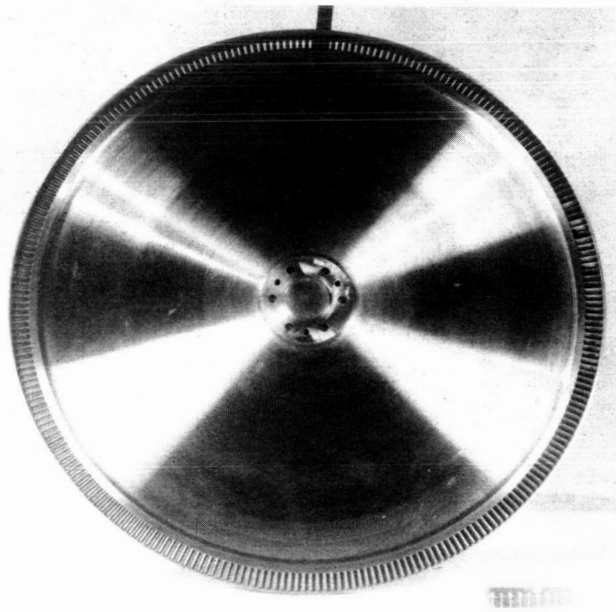


Figure 9. - Test rotor.

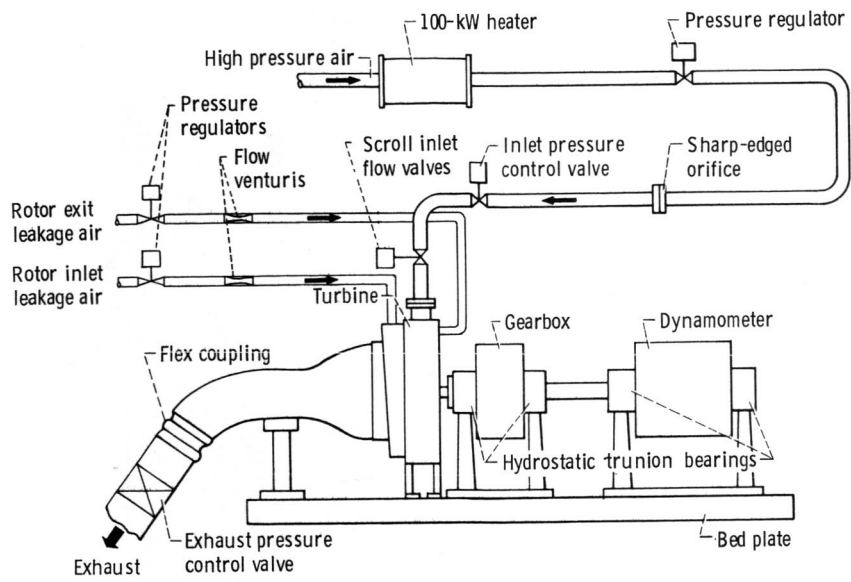


Figure 10. - Test installation diagram.

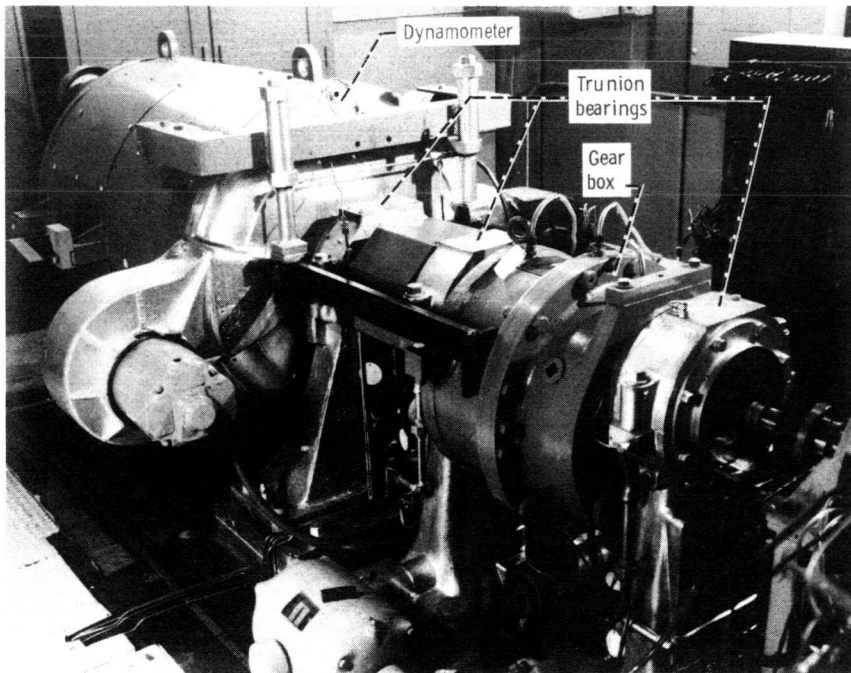


Figure 11. - Dynamometer and gear box.

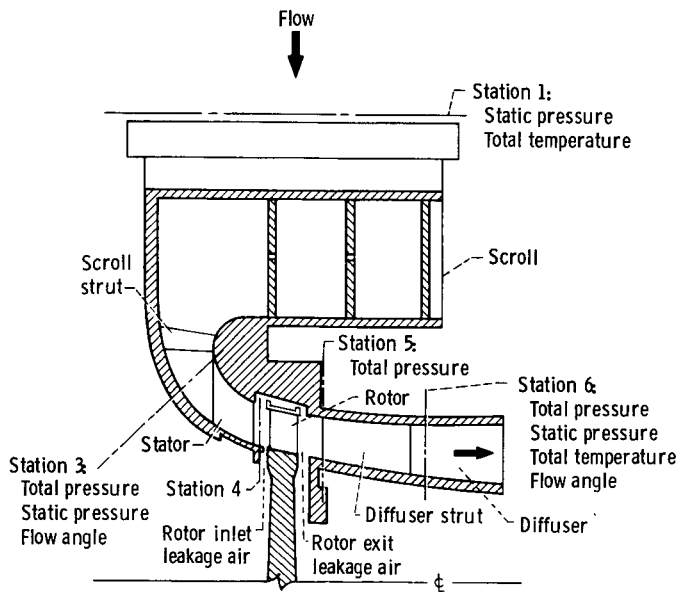


Figure 12. - Cross-sectional view of turbine.

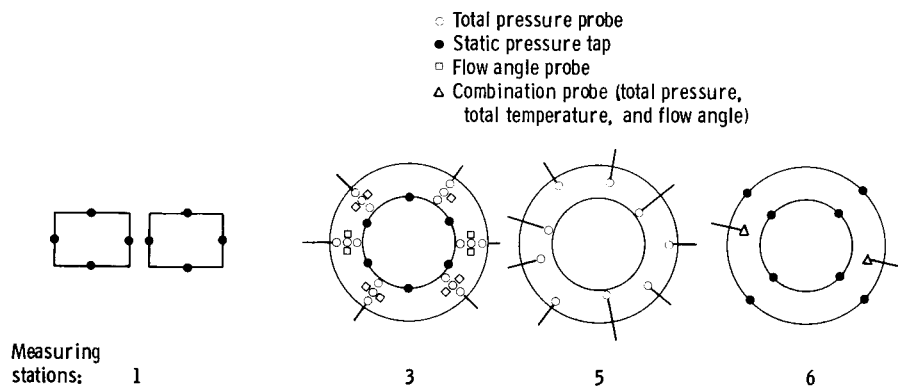


Figure 13. - Schematic of turbine instrumentation.

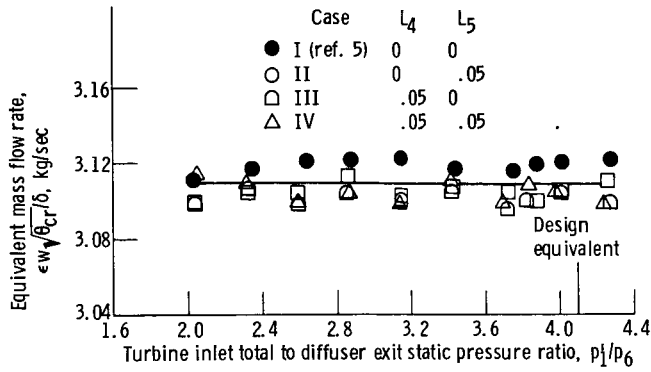


Figure 14. - Variation of mass flow rate with pressure ratio for full admission operation at design equivalent speed with simulated fan leakage air.

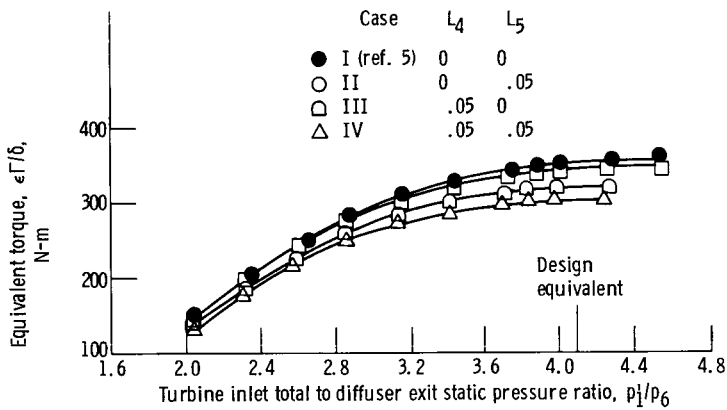


Figure 15. - Variation of torque with pressure ratio for full admission operation at design equivalent speed with simulated fan leakage air.

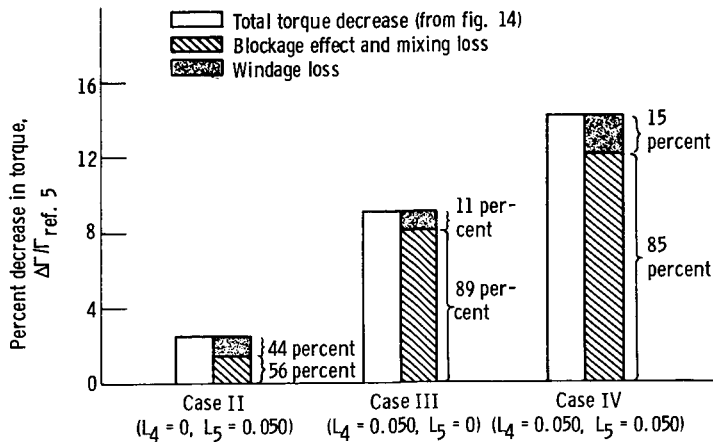


Figure 16. - Distribution of torque losses for three leakage air cases. Data at design equivalent speed and pressure ratio p_1/p_6 of 4.10.

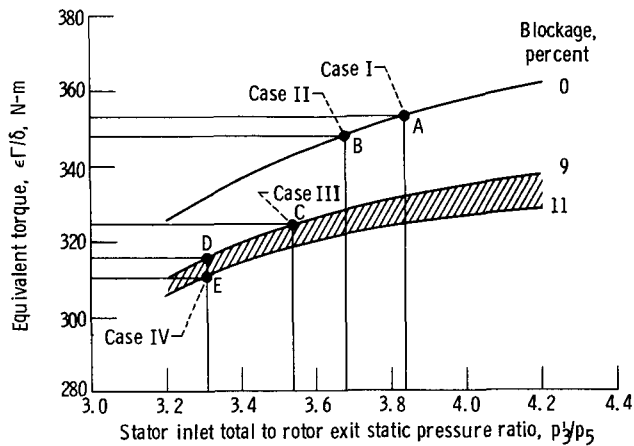


Figure 17. - Variation of torque with rotor exit static pressure for four fan leakage air cases. Results obtained from computer program of reference 8.

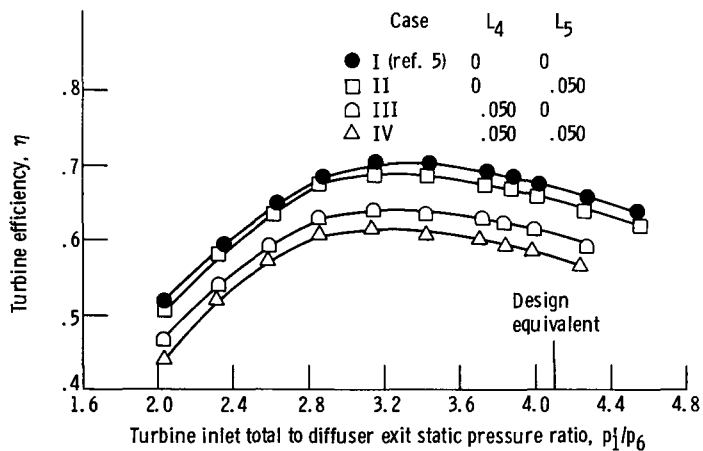
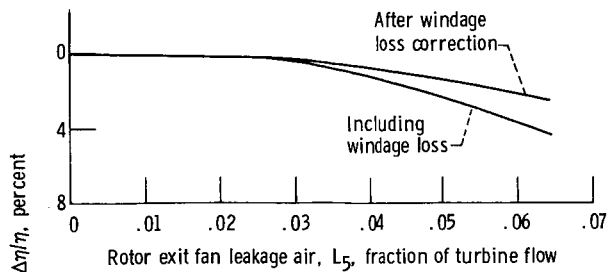
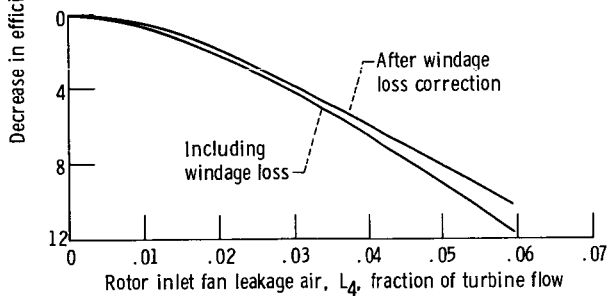


Figure 18. - Variation of efficiency with pressure ratio for full admission operation at design equivalent speed with simulated fan leakage air.



(a) Variation of rotor exit leakage air ($L_4 = 0$).



(b) Variation of rotor inlet leakage air ($L_5 = 0$).

Figure 19. - Variation of efficiency with simulated fan leakage air for full admission operation. Data at equivalent design speed and pressure ratio p_1^*/p_6 of 4.10.

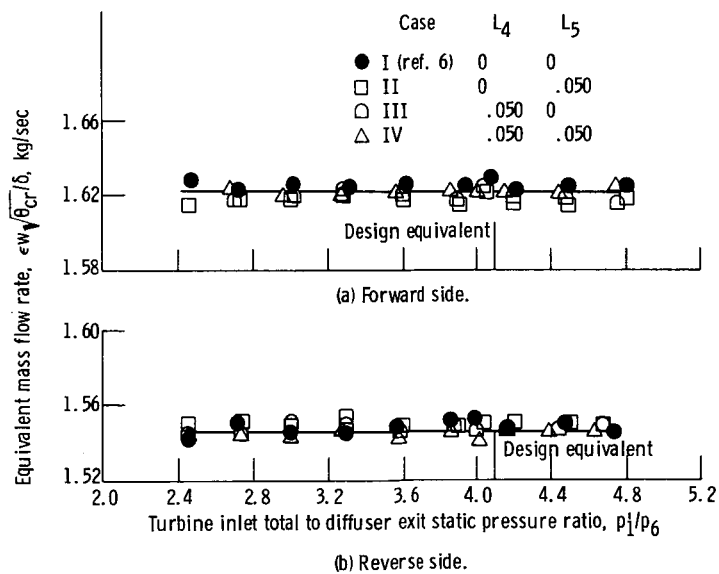


Figure 20. - Variation of mass flow rate with pressure ratio for partial admission operation at design equivalent speed with simulated fan leakage air.

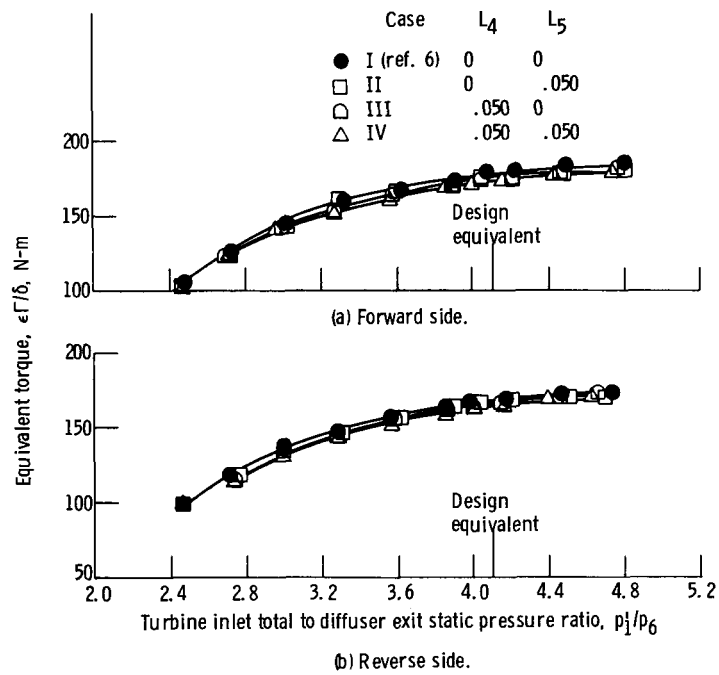


Figure 21. - Variation of torque with pressure ratio for partial admission operation at design equivalent speed with simulated fan leakage air.

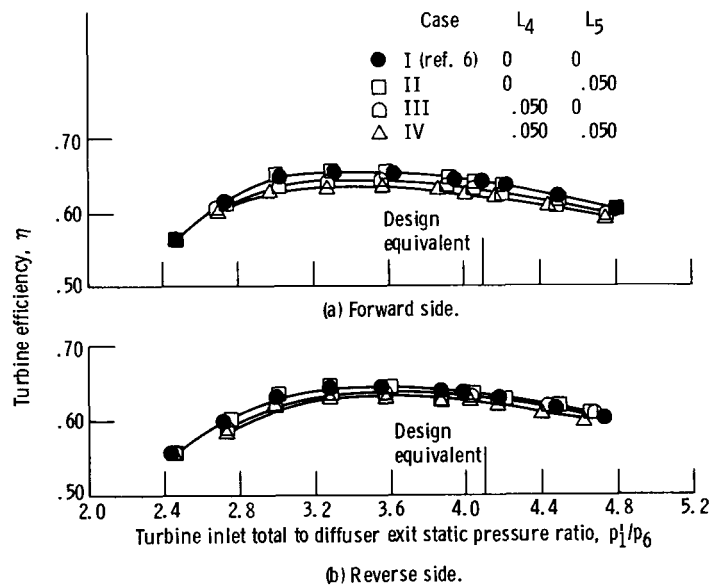


Figure 22. - Variation of efficiency with pressure ratio for partial admission operation at design equivalent speed with simulated fan leakage air.

1. Report No. NASA TP -1109		2. Government Accession No.		3. Recipient's Catalog No.	
4. Title and Subtitle COLD-AIR PERFORMANCE OF A TIP TURBINE DESIGNED TO DRIVE A LIFT FAN III - EFFECT OF SIMULATED FAN LEAKAGE ON TURBINE PERFORMANCE				5. Report Date January 1978	
				6. Performing Organization Code	
7. Author(s) Jeffrey E. Haas, Milton G. Kofskey, Glen M. Hotz, and Samuel M. Futral, Jr.				8. Performing Organization Report No. E-9331	
9. Performing Organization Name and Address NASA Lewis Research Center and Propulsion Laboratory U. S. Army R&T Laboratories (AVRADCOM) Cleveland, Ohio 44135				10. Work Unit No. 505-05	
				11. Contract or Grant No.	
12. Sponsoring Agency Name and Address National Aeronautics and Space Administration Washington, D. C. 20546				13. Type of Report and Period Covered Technical Paper	
				14. Sponsoring Agency Code	
15. Supplementary Notes					
16. Abstract <p>Performance data were obtained experimentally for a 0.4 linear scale version of the LF460 lift fan turbine for a range of scroll inlet total to diffuser exit static pressure ratios at design equivalent speed with simulated fan leakage air. Tests were conducted for full and partial admission operation with three separate combinations of rotor inlet and rotor exit leakage air. Data were compared to the results obtained from previous investigations in which no leakage air was present. Results are presented in terms of mass flow, torque, and efficiency.</p>					
17. Key Words (Suggested by Author(s)) Tip turbine; Lift fan turbine; Leakage air; Aerodynamic performance; Partial admission performance; Efficiency; VTOL aircraft; STOL aircraft			18. Distribution Statement Unclassified - unlimited STAR Category 02		
19. Security Classif. (of this report) Unclassified		20. Security Classif. (of this page) Unclassified		21. No. of Pages 27	22. Price* A00

* For sale by the National Technical Information Service, Springfield, Virginia 22161